Cite as: H. Wang *et al.*, *Science* 10.1126/science.aax7852 (2019).

CRISPR-mediated live imaging of genome editing and transcription

Haifeng Wang[1], Muneaki Nakamura[1], Timothy R. Abbott[1], Dehua Zhao[1], Kaiwen Luo[1,2], Cordelia Yu[1,3], Cindy M. Nguyen[1], Albert Lo[1], Timothy P. Daley[1,4], Marie La Russa[1], Yanxia Liu[1], Lei S. Qi[1,5,6]*

[1]Department of Bioengineering, Stanford University Stanford, CA 94305, USA. [2]ZJU-UOE Institute, Zhejiang University, School of Medicine, Haining, China. [3]Castilleja School, Palo Alto, CA 94301, USA. [4]Department of Statistics, Stanford University, Stanford, CA 94305, USA. [5]Department of Chemical and Systems Biology, Stanford University, Stanford, CA 94305, USA. [6]ChEM-H Institute, Stanford University, Stanford, CA 94305, USA.

***Corresponding author. E-mail: stanley.qi@stanford.edu**

We report a robust, versatile approach named CRISPR Live-cell fluorescent in situ hybridization (LiveFISH) using fluorescent oligos for genome tracking in broad cell types including primary cells. An intrinsic stability switch of CRISPR guide RNAs enables LiveFISH to accurately detect chromosomal disorders such as Patau Syndrome in prenatal amniotic fluid cells and track multiple loci in human T lymphocytes. In addition, LiveFISH tracks the real-time movement of DNA double-strand breaks induced by CRISPR-Cas9-mediated editing and consequent chromosome translocations. Finally, combining Cas9 and Cas13 systems, LiveFISH allows for simultaneous visualization of genomic DNA and RNA transcripts in living cells. The LiveFISH approach enables real-time live imaging of DNA and RNA during genome editing, transcription, and rearrangements in single cells.

Genome editing can induce chromosomal rearrangements including translocations (*1*, *2*). While sequencing approaches have been utilized to identify and characterize chromosomal abnormalities associated with genetic disorders and gene editing, the temporal dynamics of chromosomal rearrangements is less known. Previous studies relied on using genomic-integrated LacO/TetO arrays which is tedious and challenging (*3*). Fluorescent protein-fused, nuclease-deactivated dCas9 or single guide RNA (sgRNA) recruiting fluorescent protein-fused RNA-binding proteins enable CRISPR-mediated live imaging of genomic loci (*4*–*7*). However, DNA-encoded CRISPR components are required limiting its usage. Traditional fluorescent in situ hybridization (FISH) requires DNA denaturation, while fluorescent labeled-dCas9 assembled in vitro with sgRNA (CASFISH) detects genomic loci only in fixed samples precluding real-time tracking (*8*, *9*). Here, we report a live imaging approach, CRISPR LiveFISH, that allows real-time study of various chromosomal functions in living cells.

We first assembled equimolar amounts of dCas9-EGFP protein and Cy3-labeled guide RNA (gRNA) as fluorescent ribonucleoproteins (fRNPs), which target a repetitive region in Chromosome 3 (Chr3q29, ~500 repeats) (*4*, *5*, *7*). We delivered fRNPs into human bone osteosarcoma U2OS cells via electroporation (Fig. 1A, fig. S1A, table S1) (*10*). Flow cytometry analysis showed that more than 95% of gRNA signals were degraded within 4 hours after transfection (fig. S1B), consistent with previous reports showing that gRNAs are highly unstable in the cellular environment (*11*, *12*). However, we observed a rapid and long-lasting labeling of Cy3-gRNA at the Chr3 site, suggesting the formation of stable target-bound dCas9-gRNA complex (fig. S1C). The signal-to-background ratio (S/B) of gRNA was >4-fold higher than that of dCas9-EGFP (Fig. 1B-E, fig. S1D). Unlike dCas9-EGFP that frequently accumulated in the nucleolus, there was no nucleolar accumulation of gRNA (Fig. 1D). We performed in vitro assays and found that excessive target DNA, but not non-target DNA, protected gRNA within the Cas9:gRNA:DNA ternary complex from RNase A degradation (fig. S2A-C). In addition, dCas9-bound gRNA was better protected by fully-matched target DNA or target DNA with $\leq$4 basepairs (bp) PAM-distal mismatches than target DNAs with ≥6bp mismatches (fig. S2D-G).

Based on this target DNA-dependent protection of gRNA, we developed CRISPR LiveFISH, an approach that deploys fluorescent gRNA probes assembled with dCas9 to target and label genomic sequences in living cells (Fig. 1A). We tested CRISPR LiveFISH on cells derived from patients with Patau Syndrome, a Chr13 trisomy genetic disorder that results in organ defects, intellectual and physical impairment, and is eventually fatal (*13*). We transfected fRNPs containing dCas9 and Atto565-labeled gRNA to target a repetitive Chr13 region (Chr13q34, ~350 repeats) into normal or patient-derived prenatal amniotic fluid cells, and detected rapid and robust Chr13 labeling by Atto565-gRNA, which outperformed dCas9-EGFP RNP labeling or plasmid-based imaging (Fig. 1F-G, fig. S3A-D, movie S1, S2). The high efficiency of LiveFISH can be quantified and its accuracy was confirmed by karyotyping (fig. S3D-E, fig. S4). Simple co-delivery of fRNPs labeled with

different fluorophores enabled simultaneous visualization of repetitive Chr3 and Chr13 regions in U2OS cells (fig. S5A) and in primary human T lymphocytes (fig. S5B, movie S3). Previous methods using orthogonal dCas9s (*6*, *14*) or coupling sgRNAs to RNA aptamers and RNA binding proteins (*7*) instead require multiple constructs.

We next applied LiveFISH to study the real-time dynamics of CRISPR-Cas9-induced DNA double-strand breaks (DSBs) in living cells. We created a U2OS cell line that stably expressed a truncated 53BP1 protein (amino acid 1220-1711) fused with a fluorescent Apple protein, a well-characterized DNA DSB sensor (*15*, *16*). The human genome contains repetitive sequences that are often adjacent (<100kb) to most protein-encoding genes (>60%) (*17*). We co-delivered editing RNPs (Cas9/gPPP1R2) that cut the *PPP1R2* gene on Chr3 and LiveFISH fRNPs (Cas9/A488-gChr3) that labeled the repetitive Chr3q29 region, 36kb from the *PPP1R2* cut site, into the U2OS-53BP1-Apple cells via nucleofection (Fig. 2A, table S2). To avoid fRNP-mediated DNA cutting, we used a short (11nt) spacer for the imaging gRNA, which is insufficient for DNA cleavage (*7*, *18*). Quickly after nucleofection, we observed that a high percentage of Chr3q29 loci colocalized with 53BP1 foci in cells containing the editing gRNA (Fig. 2B-C), indicating rapid Cas9-induced DSB formation at the *PPP1R2* loci. Sequential delivery of imaging fRNPs and editing RNPs enabled us to track the process of DSB formation and 53BP1 recruitment at individual loci over time (Fig. 2D). After editing RNP delivery, we captured rapid and ongoing recruitment of 53BP1 foci to Chr3q29 loci that persisted for hours (Fig. 2E-F, table S3).

We were able to track dynamics of gene editing events. For example, we observed recruitment and subsequent dissociation of 53BP1 foci to the Chr3q29 locus, likely suggesting successful repair of DSB (Fig. 2G-H, fig. S6A). We also observed repeated recruitment and resolving of 53BP1 foci at a single DNA locus in many cells, suggesting repeated cutting and repairing of the target DNA (Fig. 2I-J, fig. S6B). Finally, multiple Chr3q29 loci clustered within the same 53BP1 foci after editing RNP delivery in some cells, indicating homologous pairing between the DSB loci as reported before (*19*) (Fig. 2K-L, fig. S6C-D). Two small 53BP1 bodies initially formed at separate Chr3q29 loci rapidly fused together, and correspondingly the homologous Chr3q29 loci interacted inside the fused 53BP1 body, suggesting that fusion of 53BP1 bodies might facilitate homologous DSB loci pairing (Fig. 2K-L, fig. S6C-D).

Using CRISPR to edit multiple genes is important for gene therapy (*20*, *21*), but can induce harmful non-homologous chromosomal rearrangements (*1*, *2*). To visualize chromosomal translocations, we co-delivered editing RNPs targeting *PPP1R2* on Chr3 and *SPACA7* on Chr13, and LiveFISH fRNPs to track both Chr3q29 and Chr13q34 (82kb from the *SPACA7* cutting site) (Fig. 3A, fig. S7A, table S2). DSB formation at targeted loci was confirmed by 53BP1 immunostaining in U2OS cells (fig. S7B), which are often aneuploid (*22*). We were able to observe the pairing of Chr3q29 and Chr13q34 loci. The two loci showed almost identical movement trajectories (movie S4) and their distance remained almost constant (Fig. 3B-C), suggesting a possible physical link between both loci. We tracked the translocation dynamics. Chr3q29 and Chr13q34 were initially separated, subsequently moved closer, and stayed together for a long period of time (Fig. 3D, fig. S8A-B, movie S5), likely representing endogenous non-homologous chromosomal translocation. We also captured transient events, wherein Chr3q29 and Chr13q34 loci moved together briefly and separated (Fig. 3E, fig. S8C). To independently confirm chromosomal translocation, we cloned, sequenced, and verified the translocated segments (fig. S9).

We further expanded CRISPR LiveFISH to image both DNA and RNA in real time. We harnessed the catalytically-deactivated Cas13d (CasRx), dCas13d, and synthesized fluorescent gRNAs for target RNA imaging (*23*). The U2OS 2-6-3 cell line harbors a repetitive LacO array upstream of Doxycycline (Dox)-inducible gene cassette containing an array of MS2 repeats (*24*) (Fig. 4A). To simultaneously visualize both DNA and RNA, we designed Atto488-labeled Cas9 gRNA to target LacO DNA (gLacO) and Atto647-labeled Cas13d gRNA to target MS2 RNA (gMS2). By co-delivery of gMS2 and dCas9/gLacO into U2OS 2-6-3 cells expressing dCas13d, we successfully labeled both DNA locus and RNA transcripts in the presence of Dox (Fig. 4B-C). CRISPR LiveFISH also enabled us to track real-time dynamics of RNA transcription in living cells. We observed gradual accumulation of MS2 transcripts around the LacO locus over time after inducing transcription with a high concentration of Dox (Fig. 4D, fig. S10).

Here, we report the CRISPR LiveFISH technology for live-cell DNA and RNA imaging. Chemically synthesized fluorescent gRNAs in complex with dCas proteins can facilitate rapid, robust, and scalable genomic DNA tracking and RNA imaging in living cells including primary cells (fig. S11, table S4). The target DNA-dependent protection of gRNAs within the Cas9:gRNA:DNA ternary complex in the RNase-rich environment enriches target signals while minimizing background noise. LiveFISH also allows dynamic tracking of CRISPR-induced gene editing and translocation events at endogenous genomic loci in living cells. Dual DNA/RNA CRISPR LiveFISH using both dCas9 and dCas13 systems enables live imaging of genomic DNA and RNA transcripts in the same cells. It is possible to combine CRISPR LiveFISH with other genetic manipulation technologies (e.g., CRISPRi/a, epigenetic modifications, and CRISPR-GO) to deepen our understanding of the spatiotemporal dynamics of genome organization and nuclear events (*5*, *17*, *25*, *26*).

REFERENCES AND NOTES

1. P. S. Choi, M. Meyerson, Targeted genomic rearrangements using CRISPR/Cas technology. *Nat. Commun.* **5**, 3728 (2014). doi:10.1038/ncomms4728 Medline
2. M. Kosicki, K. Tomberg, A. Bradley, Repair of double-strand breaks induced by CRISPR-Cas9 leads to large deletions and complex rearrangements. *Nat. Biotechnol.* **36**, 765–771 (2018). doi:10.1038/nbt.4192 Medline
3. V. Roukos, T. C. Voss, C. K. Schmidt, S. Lee, D. Wangsa, T. Misteli, Spatial dynamics of chromosome translocations in living cells. *Science* **341**, 660–664 (2013). doi:10.1126/science.1237150 Medline
4. M. Jinek, K. Chylinski, I. Fonfara, M. Hauer, J. A. Doudna, E. Charpentier, A programmable dual-RNA-guided DNA endonuclease in adaptive bacterial immunity. *Science* **337**, 816–821 (2012). doi:10.1126/science.1225829 Medline
5. B. Chen, L. A. Gilbert, B. A. Cimini, J. Schnitzbauer, W. Zhang, G.-W. Li, J. Park, E. H. Blackburn, J. S. Weissman, L. S. Qi, B. Huang, Dynamic imaging of genomic loci in living human cells by an optimized CRISPR/Cas system. *Cell* **155**, 1479–1491 (2013). doi:10.1016/j.cell.2013.12.001 Medline
6. H. Ma, A. Naseri, P. Reyes-Gutierrez, S. A. Wolfe, S. Zhang, T. Pederson, Multicolor CRISPR labeling of chromosomal loci in human cells. *Proc. Natl. Acad. Sci. U.S.A.* **112**, 3002–3007 (2015). doi:10.1073/pnas.1420024112 Medline
7. H. Ma, L.-C. Tu, A. Naseri, M. Huisman, S. Zhang, D. Grunwald, T. Pederson, Multiplexed labeling of genomic loci with dCas9 and engineered sgRNAs using CRISPRainbow. *Nat. Biotechnol.* **34**, 528–530 (2016). doi:10.1038/nbt.3526 Medline
8. P. R. Langer-Safer, M. Levine, D. C. Ward, Immunological method for mapping genes on Drosophila polytene chromosomes. *Proc. Natl. Acad. Sci. U.S.A.* **79**, 4381–4385 (1982). doi:10.1073/pnas.79.14.4381 Medline
9. W. Deng, X. Shi, R. Tjian, T. Lionnet, R. H. Singer, CASFISH: CRISPR/Cas9-mediated in situ labeling of genomic loci in fixed cells. *Proc. Natl. Acad. Sci. U.S.A.* **112**, 11870–11875 (2015). doi:10.1073/pnas.1515692112 Medline
10. X. Liang, J. Potter, S. Kumar, Y. Zou, R. Quintanilla, M. Sridharan, J. Carte, W. Chen, N. Roark, S. Ranganathan, N. Ravinder, J. D. Chesnut, Rapid and highly efficient mammalian cell engineering via Cas9 protein transfection. *J. Biotechnol.* **208**, 44–53 (2015). doi:10.1016/j.jbiotec.2015.04.024 Medline
11. H. Ma, L.-C. Tu, A. Naseri, M. Huisman, S. Zhang, D. Grunwald, T. Pederson, CRISPR-Cas9 nuclear dynamics and target recognition in living cells. *J. Cell Biol.* **214**, 529–537 (2016). doi:10.1083/jcb.201604115 Medline
12. A. Hendel, R. O. Bak, J. T. Clark, A. B. Kennedy, D. E. Ryan, S. Roy, I. Steinfeld, B. D. Lunstad, R. J. Kaiser, A. B. Wilkens, R. Bacchetta, A. Tsalenko, D. Dellinger, L. Bruhn, M. H. Porteus, Chemically modified guide RNAs enhance CRISPR-Cas genome editing in human primary cells. *Nat. Biotechnol.* **33**, 985–989 (2015). doi:10.1038/nbt.3290 Medline
13. B. J. Baty, B. L. Blackburn, J. C. Carey, Natural history of trisomy 18 and trisomy 13: I. Growth, physical assessment, medical histories, survival, and recurrence risk. *Am. J. Med. Genet.* **49**, 175–188 (1994). doi:10.1002/ajmg.1320490204 Medline
14. B. Chen, J. Hu, R. Almeida, H. Liu, S. Balakrishnan, C. Covill-Cooke, W. A. Lim, B. Huang, Expanding the CRISPR imaging toolset with Staphylococcus aureus Cas9 for simultaneous imaging of multiple genomic loci. *Nucleic Acids Res.* **44**, e75 (2016). doi:10.1093/nar/gkv1533 Medline
15. K. S. Yang, R. H. Kohler, M. Landon, R. Giedt, R. Weissleder, Single cell resolution in vivo imaging of DNA damage following PARP inhibition. *Sci. Rep.* **5**, 10129 (2015). doi:10.1038/srep10129 Medline
16. Y. Huyen, O. Zgheib, R. A. Ditullio Jr., V. G. Gorgoulis, P. Zacharatos, T. J. Petty, E. A. Sheston, H. S. Mellert, E. S. Stavridi, T. D. Halazonetis, Methylated lysine 79 of histone H3 targets 53BP1 to DNA double-strand breaks. *Nature* **432**, 406–411 (2004). doi:10.1038/nature03114 Medline
17. H. Wang, X. Xu, C. M. Nguyen, Y. Liu, Y. Gao, X. Lin, T. Daley, N. H. Kipniss, M. La Russa, L. S. Qi, CRISPR-Mediated Programmable 3D Genome Positioning and Nuclear Organization. *Cell* **175**, 1405–1417.e14 (2018). doi:10.1016/j.cell.2018.09.013 Medline
18. H. K. Liao, F. Hatanaka, T. Araoka, P. Reddy, M.-Z. Wu, Y. Sui, T. Yamauchi, M. Sakurai, D. D. O'Keefe, E. Núñez-Delicado, P. Guillen, J. M. Campistol, C.-J. Wu, L.-F. Lu, C. R. Esteban, J. C. Izpisua Belmonte, In Vivo Target Gene Activation via CRISPR/Cas9-Mediated Trans-epigenetic Modulation. *Cell* **171**, 1495–1507.e15 (2017). doi:10.1016/j.cell.2017.10.025 Medline
19. M. Gandhi, V. N. Evdokimova, K. T Cuenco, M. N. Nikiforova, L. M. Kelly, J. R. Stringer, C. J. Bakkenist, Y. E. Nikiforov, Homologous chromosomes make contact at the sites of double-strand breaks in genes in somatic G_0/G_1-phase human cells. *Proc. Natl. Acad. Sci. U.S.A.* **109**, 9454–9459 (2012). doi:10.1073/pnas.1205759109 Medline
20. J. Ren, X. Zhang, X. Liu, C. Fang, S. Jiang, C. H. June, Y. Zhao, A versatile system for rapid multiplex genome-edited CAR T cell generation. *Oncotarget* **8**, 17002–17011 (2017). Medline
21. S. Mattapally, K. M. Pawlik, V. G. Fast, E. Zumaquero, F. E. Lund, T. D. Randall, T. M. Townes, J. Zhang, Human Leukocyte Antigen Class I and II Knockout Human Induced Pluripotent Stem Cell-Derived Cells: Universal Donor for Cell Therapy. *J. Am. Heart Assoc.* **7**, e010239 (2018). doi:10.1161/JAHA.118.010239 Medline
22. K. Al-Romaih, J. Bayani, J. Vorobyova, J. Karaskova, P. C. Park, M. Zielenska, J. A. Squire, Chromosomal instability in osteosarcoma and its association with centrosome abnormalities. *Cancer Genet. Cytogenet.* **144**, 91–99 (2003). doi:10.1016/S0165-4608(02)00929-9 Medline
23. S. Konermann, P. Lotfy, N. J. Brideau, J. Oki, M. N. Shokhirev, P. D. Hsu, Transcriptome Engineering with RNA-Targeting Type VI-D CRISPR Effectors. *Cell* **173**, 665–676.e14 (2018). doi:10.1016/j.cell.2018.02.033 Medline
24. S. M. Janicki, T. Tsukamoto, S. E. Salghetti, W. P. Tansey, R. Sachidanandam, K. V. Prasanth, T. Ried, Y. Shav-Tal, E. Bertrand, R. H. Singer, D. L. Spector, From silencing to gene expression: Real-time analysis in single cells. *Cell* **116**, 683–698 (2004). doi:10.1016/S0092-8674(04)00171-0 Medline
25. L. S. Qi, M. H. Larson, L. A. Gilbert, J. A. Doudna, J. S. Weissman, A. P. Arkin, W. A. Lim, Repurposing CRISPR as an RNA-guided platform for sequence-specific control of gene expression. *Cell* **152**, 1173–1183 (2013). doi:10.1016/j.cell.2013.02.022 Medline
26. I. B. Hilton, A. M. D'Ippolito, C. M. Vockley, P. I. Thakore, G. E. Crawford, T. E. Reddy, C. A. Gersbach, Epigenome editing by a CRISPR-Cas9-based acetyltransferase activates genes from promoters and enhancers. *Nat. Biotechnol.* **33**, 510–517 (2015). doi:10.1038/nbt.3199 Medline
27. M. Jinek, F. Jiang, D. W. Taylor, S. H. Sternberg, E. Kaya, E. Ma, C. Anders, M. Hauer, K. Zhou, S. Lin, M. Kaplan, A. T. Iavarone, E. Charpentier, E. Nogales, J. A. Doudna, Structures of Cas9 endonucleases reveal RNA-mediated conformational activation. *Science* **343**, 1247997 (2014). doi:10.1126/science.1247997 Medline
28. F. Jiang, D. W. Taylor, J. S. Chen, J. E. Kornfeld, K. Zhou, A. J. Thompson, E. Nogales, J. A. Doudna, Structures of a CRISPR-Cas9 R-loop complex primed for DNA cleavage. *Science* **351**, 867–871 (2016). doi:10.1126/science.aad8282 Medline
29. S. Lin, B. T. Staahl, R. K. Alla, J. A. Doudna, Enhanced homology-directed human genome engineering by controlled timing of CRISPR/Cas9 delivery. *eLife* **3**, e04766 (2014). doi:10.7554/eLife.04766 Medline
30. J. Schindelin, I. Arganda-Carreras, E. Frise, V. Kaynig, M. Longair, T. Pietzsch, S. Preibisch, C. Rueden, S. Saalfeld, B. Schmid, J.-Y. Tinevez, D. J. White, V. Hartenstein, K. Eliceiri, P. Tomancak, A. Cardona, Fiji: An open-source platform for biological-image analysis. *Nat. Methods* **9**, 676–682 (2012). doi:10.1038/nmeth.2019 Medline
31. P. Qin, M. Parlak, C. Kuscu, J. Bandaria, M. Mir, K. Szlachta, R. Singh, X. Darzacq, A. Yildiz, M. Adli, Live cell imaging of low- and non-repetitive chromosome loci using CRISPR-Cas9. *Nat. Commun.* **8**, 14725 (2017). doi:10.1038/ncomms14725 Medline

ACKNOWLEDGMENTS

We thank Stanford Cytogenetics Laboratory for karyotyping, Stanford Shared FACS Facilities for cell sorting, the Cell Sciences Imaging Facility and Cedric Espenel for microscope usage, ChEM-H Macromolecular Structure Knowledge Center for protein purification, Dr. David L. Spector in Cold Spring Harbor Laboratory for U2OS 2-6-3 cells, and Coriell Cell Repositories for amniotic fluid cell samples. **Funding**: T.R.A. acknowledges support from NSF GRFP. L.S.Q acknowledges the funding support from the Li Ka Shing Foundation. Part of the work is supported by the National Institutes of Health Common Fund 4D Nucleome Program (U01 EB021240), the Pew Scholar Foundation, and the Alfred P. Sloan Foundation. **Author contributions:** H.W. and L.S.Q. conceived the study. H.W. and L.S.Q. designed the experiments. H.W., M.N., T.R.A., D.Z., K.L., C.Y., C.M.N., A.L., and Y.L. performed the experiments. H.W., K.L., C.M.N., T.P.D., and L.S.Q. analyzed

the data. H.W., M.L. and L.S.Q wrote the manuscript with help from all authors.
Competing interests: H.W. and L.S.Q. are co-inventors of a patent filed by Stanford University on related work (US provisional patent No. 29/393,761).
Data and materials availability: All data are available in the manuscript or the supplementary materials. Plasmids are available on Addgene.

SUPPLEMENTARY MATERIALS

science.sciencemag.org/cgi/content/full/science.aax7852/DC1
Materials and Methods
Figs. S1 to S11
Tables S1 to S4
References (*27*–*31*)
Movies S1 to S5

22 April 2019; accepted 19 August 2019
Published online 5 September 2019
10.1126/science.aax7852

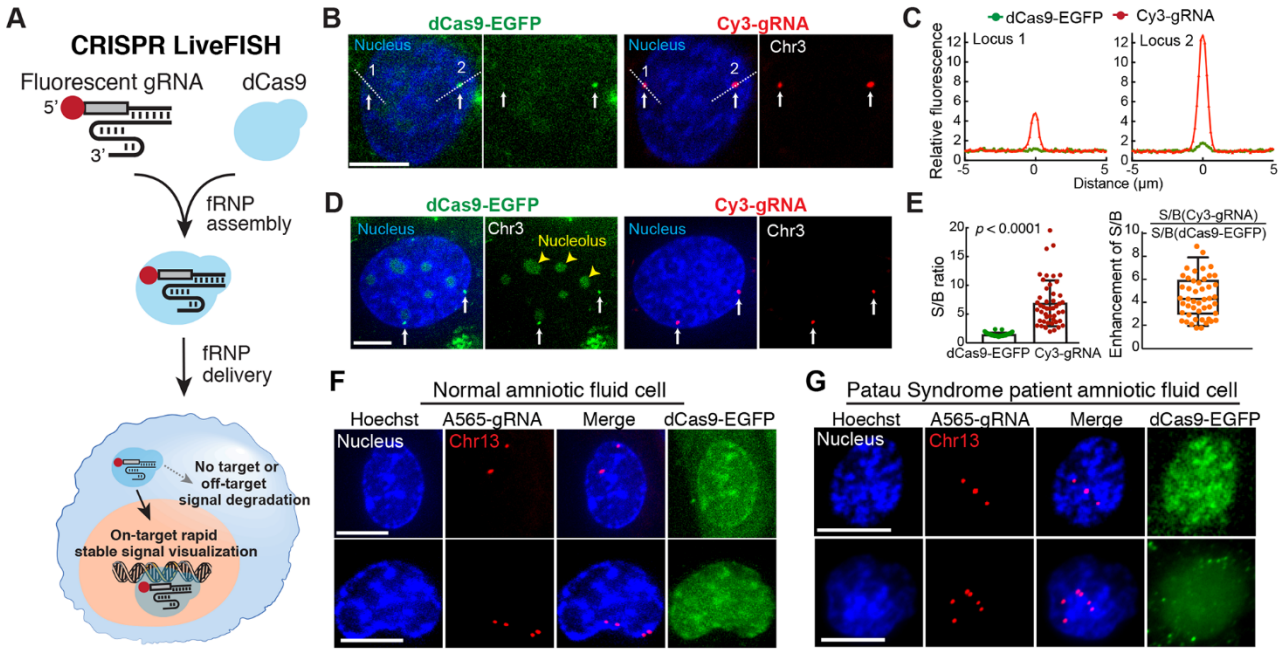

Fig. 1. DNA target-dependent protection of gRNA enables LiveFISH for robust genomic tracking and cytogenetic diagnosis in primary cells. (**A**) Schematic of LiveFISH for genomic imaging and cytogenetic detection in living cells via fluorescent ribonucleoprotein (fRNP) consisting of synthesized fluorescent gRNA and dCas9. (**B-D**) Comparison of fluorescent gRNA (Cy3-gRNA, red) and dCas9-EGFP (green) labeling a repetitive Chr3q29 locus (white arrows) in U2OS cells via fRNP delivery. The dotted lines in (**B**) are used for linescan in (**C**) The yellow arrowheads in (**D**) show nucleolar dCas9-EGFP accumulation. (**E**) Comparison of signal-to-background ratio (S/B) of labeled Chr3q29 loci using fluorescent gRNA (red) and dCas9-EGFP (green). Left, mean ± SD and $p<0.0001$ by t-test; right, the box plot of calculated ratios (orange) between the S/B of Cy3-gRNA and dCas9-EGFP at each locus. (**F-G**) Images of LiveFISH imaging and cytogenetic detection in normal (**F**) and Patau Syndrome patient-derived (**G**) amniotic fluid cells with fRNP containing dCas9-EGFP (green) and Atto565-gRNA (red) targeting Chr13. See movies S1 and S2 for dynamics. Scale bars, 10 μm.

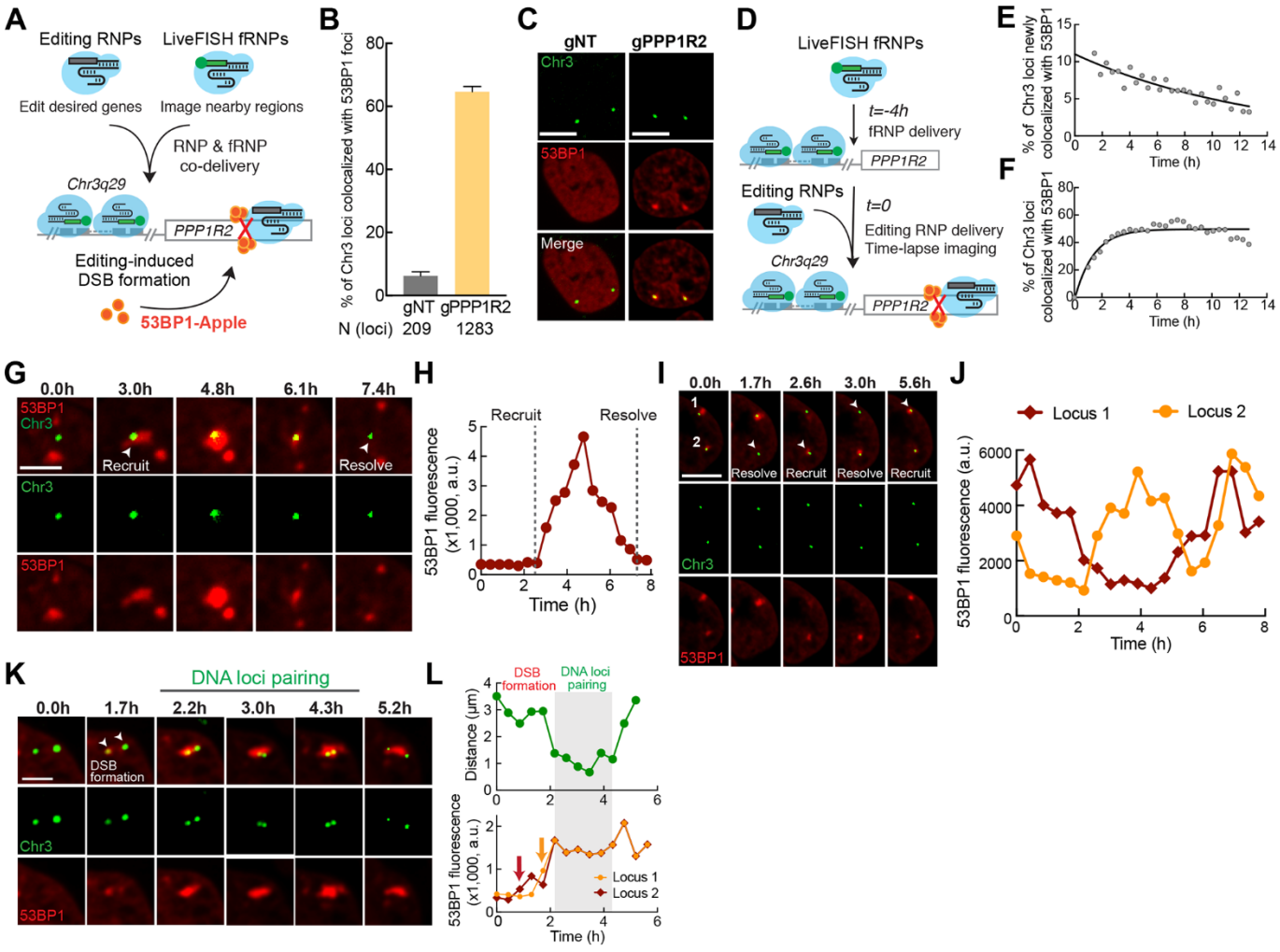

Fig. 2. LiveFISH real-time visualization of gene-editing-induced DNA double-strand breaks (DSBs) in living cells. (**A**) Schematic of visualizing gene-editing-induced DSB dynamics by co-delivering LiveFISH fRNPs and CRISPR editing RNPs in 53BP1-Apple U2OS cells. (**B**) Percentages of 53BP1-colocalized Chr3 loci using a non-targeting gRNA (gNT) and a *PPP1R2*-targeting gRNA (gPPP1R2). Data shows mean ± SEM. $p<0.0001$ by Fisher's exact test. (**C**) Representative images comparing localization of 53BP1 and Chr3 loci in cells with gNT and gPPP1R2. Scale bars, 10 μm. (**D**) Schematic of visualizing gene-editing-induced DSB dynamics by sequentially delivering LiveFISH fRNPs (t=-4h) and editing RNPs (t=0). (**E-F**) Percentages of newly (**E**) and total (**F**) 53BP1-colocalized Chr3q29 loci over time after editing RNP delivery (t=0). Black lines show non-linear fits. (**G-H**) Representative images (**G**) and quantification of 53BP1 fluorescence (**H**) at Chr3q29 loci during gene editing. (**I-J**) Representative images (**I**) and quantification of 53BP1 fluorescence (**J**) during repeated recruitment and resolution of 53BP1 at Chr3q29 loci. (**K-L**) Representative images (**K**) and quantification of distance between the Chr3 loci (**L**, top) and 53BP1 fluorescence (**L**, bottom) during 53BP1 loci fusion and homologous Chr3 loci pairing. Colored arrows in **L** indicate 53BP1 foci formation. White arrowheads in (**G**, **I**, and **K**) show 53BP1 recruiting or resolving events; a.u., arbitrary unit. Scale bars, 5 μm.

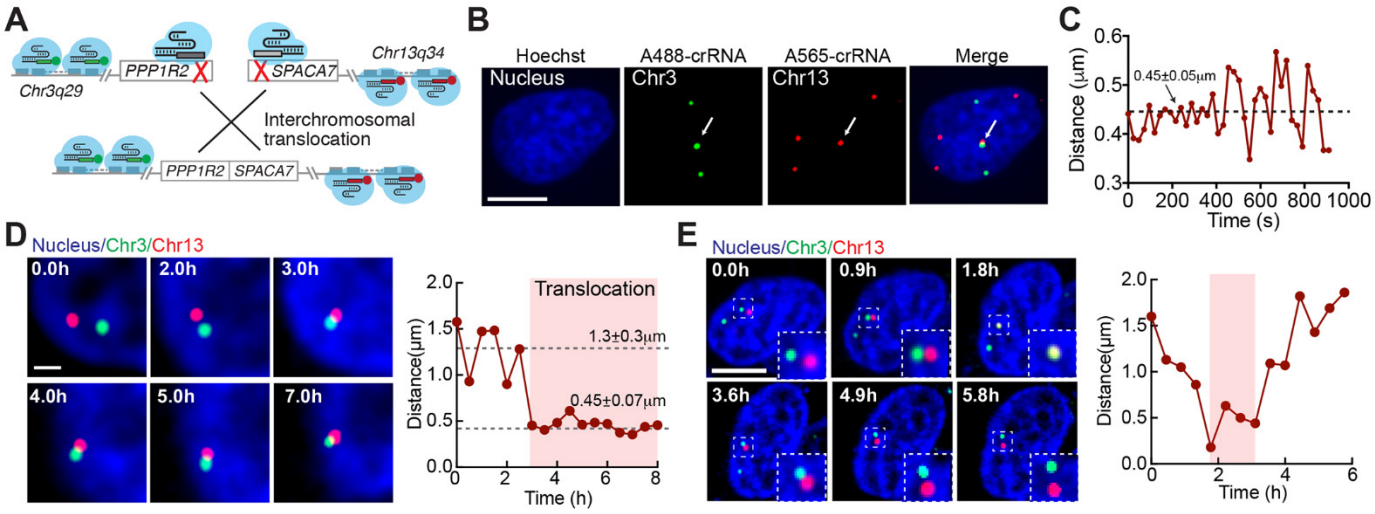

Fig. 3. LiveFISH detection and visualization of gene-editing-induced chromosome translocations in living cells. (**A**) Schematic of visualizing chromosomal translocations using LiveFISH fRNPs and CRISPR editing RNPs. (**B-C**) A representative U2OS cell (**B**) showing a pair of co-localized Chr3/Chr13 loci (arrow) and quantification of the Chr3/Chr13 distance (**C**) over a short time. See movie S4 for dynamics. (**D**) Representative images showing chromosomal translocation formation between Chr13 and Chr3 and distance over time. See movie S5 for dynamics. Scale bar, 1 μm. (**E**) Representative images showing transient colocalization between Chr13/Chr3 (outlined in white boxes) and distance over time. Scale bar, 10 μm.

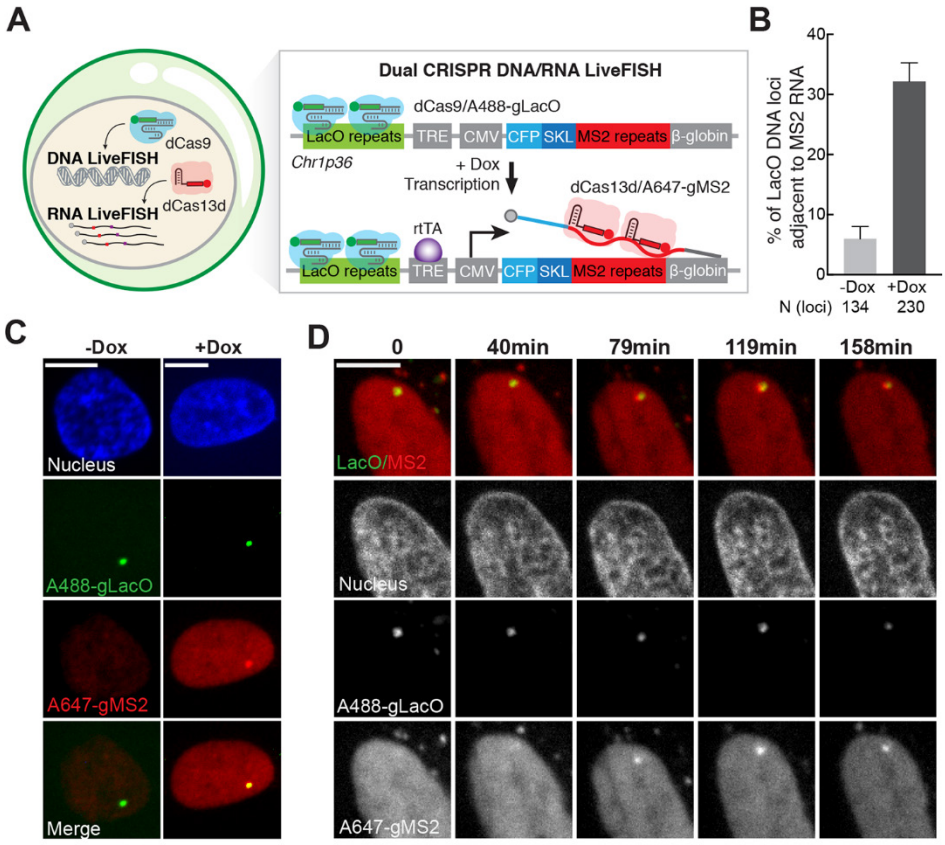

Fig. 4. Dual CRISPR DNA/RNA LiveFISH enables real-time visualization of transcription in living cells. (**A**) Schematic of dual DNA/RNA LiveFISH in living cells. (**B-C**) Percentages of LacO DNA loci showing adjacent labeled MS2 RNA -/+ Dox (**B**) and representative images (**C**). (**D**) Representative images showing MS2 mRNA transcription dynamics after adding a high concentration of Dox.

CRISPR-mediated live imaging of genome editing and transcription

Haifeng Wang, Muneaki Nakamura, Timothy R. Abbott, Dehua Zhao, Kaiwen Luo, Cordelia Yu, Cindy M. Nguyen, Albert Lo, Timothy P. Daley, Marie La Russa, Yanxia Liu and Lei S. Qi

published online September 5, 2019